Metabolic Engineering 17 (2013) 12–22

Contents lists available at SciVerse ScienceDirect

Metabolic Engineering

journal homepage: www.elsevier.com/locate/ymben

Synergy as design principle for metabolic engineering of 1-propanol production in *Escherichia coli*

Claire R. Shen [a,b], James C. Liao [a,b,*]

[a] Department of Chemical and Biomolecular Engineering, University of California, Los Angeles 5531 Boelter Hall, Los Angeles, CA 90095, USA
[b] Institute for Genomics and Proteomics, University of California, Los Angeles 5531 Boelter Hall, Los Angeles, CA 90095, USA

ARTICLE INFO

Article history:
Received 5 November 2012
Received in revised form
4 January 2013
Accepted 24 January 2013
Available online 31 January 2013

Keywords:
Metabolic engineering
Biofuel
Synergy
Synthetic biology

ABSTRACT

Synthesis of a desired product can often be achieved via more than one metabolic pathway. Whether naturally evolved or synthetically engineered, these pathways often exhibit specific properties that are suitable for production under distinct conditions and host organisms. Synergy between pathways arises when the underlying pathway characteristics, such as reducing equivalent demand, ATP requirement, intermediate utilization, and cofactor preferences, are complementary to each other. Utilization of such pathways in combination leads to an increased metabolite productivity and/or yield compared to using each pathway alone. This work illustrates the principle of synergy between two different pathways for 1-propanol production in *Escherichia coli*. A model-guided design based on maximum theoretical yield calculations identified synergy of the native threonine pathway and the heterologous citramalate pathway in terms of production yield across all flux ratios between the two pathways. Characterization of the individual pathways by host gene deletions demonstrates their distinct metabolic characteristics: the necessity of TCA cycle for threonine pathway and the independence of TCA cycle for the citramalate pathway. The two pathways are also complementary in driving force demands. Production experiments verified the synergistic effects predicted by the yield model, in which the platform with dual pathway for 2-ketobutyrate synthesis achieved higher yield (0.15 g/g of glucose) and productivity (0.12 g/L/h) of 1-propanol than individual ones alone: the threonine pathway (0.09 g/g; 0.04 g/L/h) or the citramalate pathway (0.11 g/g; 0.04 g/L/h). Thus, incorporation of synergy into the design principle of metabolic engineering may improve the production yield and rate of the desired compound.

1. Introduction

Pathway design is one of the most important aspects in metabolic engineering to achieve high product yield under desirable operating conditions in a given host organism. In the global network of metabolic pathways, a particular metabolite can often be produced by more than one pathway. Whether the pathways are naturally present in the host organism or synthetically created by linking steps of unrelated reactions, they may possess unique characteristics in terms of precursor availability, cofactor preference, ATP and reducing power demand, oxygen requirement, and maximum theoretical yield. For example, production of 1-butanol in *Escherichia coli* has been demonstrated from two distinct pathways Lan and Liao, in press, one via the fermentative Coenzyme A (CoA) dependent pathway following the reaction sequence of reverse β-oxidation (Atsumi et al., 2008a; Bond-Watts et al., 2011; Dellomonaco et al., 2011), and the other one via the non-fermentative ketoacid pathway following the chemistry scheme of norvaline biosynthesis (Atsumi et al., 2008b; Shen and Liao, 2008). Each pathway differs in its cofactor preference and ATP requirement. In *E. coli*, high titer production of 1-butanol was achieved anaerobically using the CoA-dependent pathway via accumulation of NADH and acetyl-CoA as driving forces (Shen et al., 2011). Nonetheless, as the host organism switched from *E. coli* to the strict aerobic cyanobacteria *Synechococcus elongatus* PCC 7942, the same type of driving force no longer applied Lan and Liao., 2011. Direct photosynthetic production of 1-butanol from CO_2 could only be achieved in *S. elongatus* PCC 7942 by synthetically re-routing the CoA pathway via malonyl-CoA synthesis to utilize ATP consumption as a driving force (Lan and Liao, 2012). Characteristics of a pathway therefore can be advantageous or disadvantageous to the product formation depending on the target host and culturing condition. In some cases, complementary nature of the distinct pathways may lead to synergistic effects which reflect in the production rate and yield. This work examines pathway synergy as a design principle in metabolic engineering using 1-propanol production as an example.

* Corresponding author at: University of California, Department of Chemical and Biomolecular Engineering, 5531 Boelter Hall, Los Angeles, CA 90095-1592, USA. Fax: +1 310 206 4107.
E-mail addresses: liaoj@ucla.edu, liaoj@seas.ucla.edu (J.C. Liao).

1096-7176/$ - see front matter © 2013 Elsevier Inc. All rights reserved.
http://dx.doi.org/10.1016/j.ymben.2013.01.008

There are two pathways leading to the synthesis of 1-propanol precursor 2-ketobutyrate (2KB): the threonine pathway and the citramalate pathway. 2-Ketobutyrate is an important metabolite leading to the production of many higher-chain alcohols (Cann and Liao, 2008; Zhang et al., 2008) and certain hydroxyacids (Tseng et al., 2010) which serve as important building blocks for biodegradable polyhydroxyalkanoates. 1-Propanol is another compound produced from 2-ketobutyrate that is industrially important both as a C_3 chemical feedstock and in energy applications. 1-Propanol can be dehydrated to yield propylene, a raw material for polypropylene which constitutes a major portion of plastic material. It can also replace methanol in the transesterification reaction to avoid the use of organic solvents during the production of biodiesel fuel with immobilized lipase (Iso et al., 2001). 1-Propanol is currently produced from the petrochemical feedstock ethylene and is used as a multi-purpose solvent in a variety of industrial products such as paint, cleaner and cosmetics.

Previously, we had demonstrated the co-production of 1-propanol and 1-butanol in *E. coli* (Fig. 1a) via the native threonine biosynthetic pathway (Shen and Liao, 2008) and the heterologous citramalate pathway (Atsumi and Liao, 2008). Deregulation of threonine biosynthesis by the feedback resistant aspartate kinase ($ThrA^{fbr}$) and elimination of divergent pathways catalyzed by *metA*, *tdh*, *ilvBN*, *ilvIH*, and *adhE* resulted in a final production titer of 2 g/L from the threonine pathway, with nearly 1:1 ratio of 1-propanol and 1-butanol (Shen and Liao, 2008). On the other hand, directed evolution of the *Methanococcus jannaschii* citramalate synthase (CimA) via selection in the isoleucine auxotroph SA405 (JCL16 Δ*ilvA* Δ*tdcB*) led to a production titer of 3.5 g/L of 1-propanol and 0.5 g/L of 1-butanol from the engineered citramalate pathway (Atsumi and Liao, 2008). A novel dehydratase-mediated pathway for 1-propanol production via 1,2-propandiol has also been reported recently (Jain and Yan, 2011).

Branching off from oxaloacetate (OAA), the threonine biosynthetic pathway initiates with the formation of aspartate via transamination of OAA by the aspartate aminotransferase (AspC) at the expense of one glutamate (Fig. 1a). Through a series of reactions catalyzed by the aspartate kinase (ThrA, MetL, lysC), aspartate semialdehyde dehydrogenase (Asd), homoserine kinase (ThrB), and threonine synthase (ThrC), threonine is generated from aspartate with the consumption of two ATP and two NADPH. Then, the essential 1-propanol precursor 2-ketobutyrate is produced via deamination of threonine by the threonine deaminase (IlvA) and/or the biodegradative threonine dehydratase (TdcB). The advantage provided by the fixation of carbon dioxide during OAA formation is compromised by the high demand of reducing power from the threonine pathway.

Citramalate pathway, found in mostly methanogenic archaea such as *Methanococcus jannaschii* and certain bacteria such as

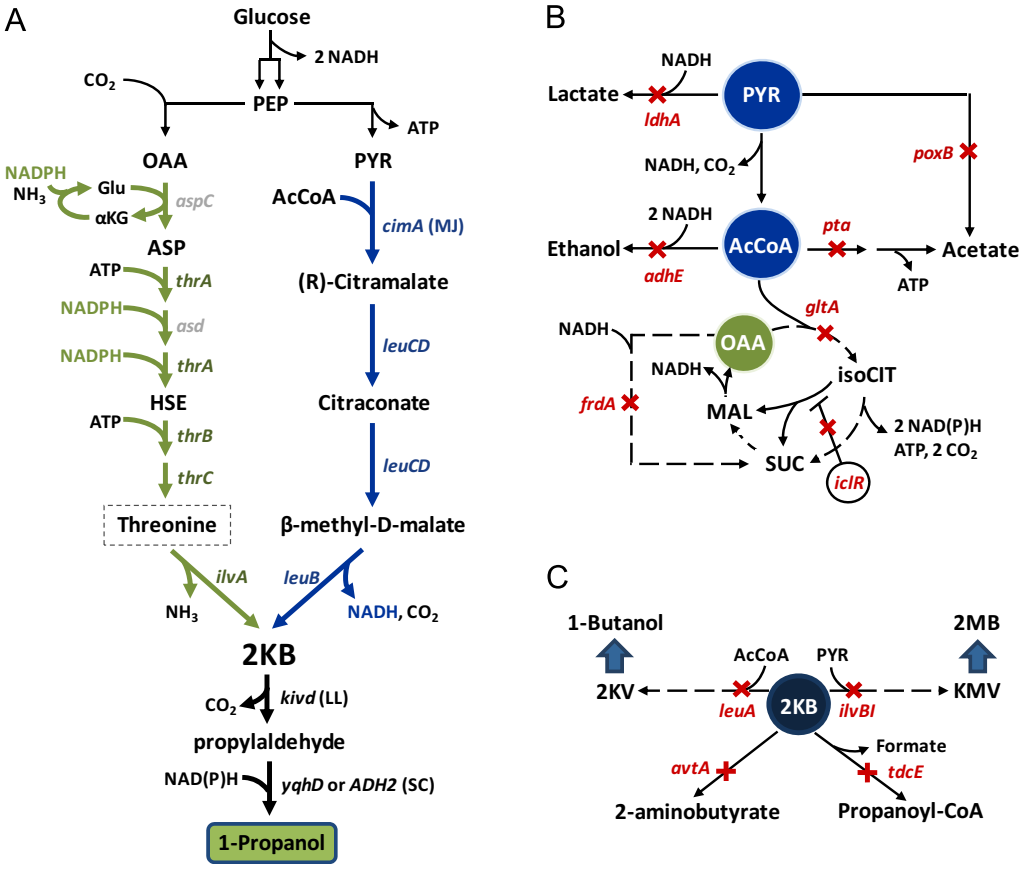

Fig. 1. Schematic illustration of the threonine pathway, the citramalate pathway, and the host gene deletions for the synthesis of 1-propanol in *E. coli*. (A) Illustration of the dual pathway leading to the production of 2-ketobutyrate. The native threonine pathway is denoted by the green arrows while the heterologous citramalate pathway is denoted by the blue arrows. Foreign genes are followed by initials of the organism. Genes not overexpressed are noted in gray font. (B) Host gene deletions for the characterization of 1-propanol production. Genes deleted are shown in red next to the crosses. (C) Conservation of the 2-ketobutyrate pool by host gene deletions. MJ, *Methanococcus jannaschii*; LL, *Lactococcus lactis; SC, Saccharomyces cerevisiae*; 2KB, 2-ketobutyrate; 2KV, 2-ketovalerate; KMV, 2-keto-3-methylvalerate; AcCoA, acetyl-CoA; PYR, pyruvate; PEP, phosphoenolpyruvate; OAA, oxaloacetate; ASP, aspartate. Glu, glutamate; αKG, α-ketoglutarate; HSE, homoserine; isoCIT, isocitrate; MAL, malate; SUC, succinate. (For interpretation of the references to color in this figure legend, the reader is referred to the web version of this article.)

Leptospira interrogans, is an alternative route which bypasses threonine biosynthesis to generate 2-ketobutyrate. Parallel to the reaction schemes found in the iterative ketoacid elongation catalyzed by enzymes LeuABCD (Shen and Liao, 2011; Zhang et al., 2008), synthesis of 2-ketobutyrate initiates with the condensation of acetyl-CoA and pyruvate catalyzed by the citramalate synthase CimA, a structural homologue of LeuA. The resulting product (R)-citramalate is subsequently converted into 2-ketobutyrate via the promiscuity of enzymes LeuBCD (Fig. 1a). In contrast to the threonine pathway, the citramalate pathway generates one net NADH which can be applied to the 1-propanol production. In addition, the last decarboxylation step catalyzed by LeuB may provide an irreversible driving force to drive carbon flux towards the synthesis of 2-ketobutyrate.

This study focuses on the synergy of the threonine pathway and the citramalate pathway in the production of 1-propanol. First, theoretical yield calculation was used to characterize the individual ketoacid pathways and identify the existence of synergy in terms of production yield. Then, the synergistic effect on the yield was demonstrated by the strain containing both pathways for 2-ketobutyrate synthesis, which achieved 30–50% higher yield of 1-propanol than the strains containing each individual pathway separately. Although the theoretical yield calculation does not predict synergy in productivity, presence of the dual pathway successfully improved the 1-propanol production rate. We propose synergy as a design principle that is generalizable to other metabolic systems.

2. Materials and methods

2.1. Reagents

Restriction enzymes and Antarctic phosphatase were purchased from New England Biolabs (Ipswich, MA). Rapid DNA ligation kit was from Roche (Mannheim, Germany). KOD DNA polymerase was from EMD Chemicals (San Diego, CA). Oligonucleotides were purchased from IDT (San Diego, CA) or Operon (Huntsville, AL). All chemicals used were obtained from Sigma-Aldrich (St. Louis, MO) or Fisher Scientifics (Pittsburgh, PA) unless specified otherwise.

2.2. Plasmid construction

Plasmid pCS31 was made by amplifying *ilvA* from *E. coli* BW25113 WT genomic DNA with primers A110 and A112 (Atsumi et al., 2008b), cut with *Acc65* and *XhoI* and ligated into pCS27 (Shen and Liao, 2008) cut with the same enzymes. Plasmids pCS72 was made by amplifying the *thrA*^{fbr}*BC* operon from pCS49, digested, and ligated behind *ilvA* into the pCS31 open vector cut with the same pair of enzymes. Plasmids pCS86 was made by amplifying the *gltA* gene from *E. coli* WT genomic DNA using primers given in Table 1, digested, and ligated into the pCS49 open vector cut with the same pair of enzymes.

Table 1
Strains, plasmids, and primers used.

Strain	Genotype	Reference
BW25113	*rrnB*$_{T14}$ Δ*lacZ*$_{WJ16}$ *hsdR*514 Δ*araBAD*$_{AH33}$ Δ*rhaBAD*$_{LD78}$	(Datsenko and Wanner, 2000)
XL-1 Blue	*recA1 endA1 gyrA96 thi-1 hsdR17 supE44 relA1 lac* [F' *proAB lacI*^{q}*ZΔM15 Tn10* (Tet^R)]	Stratagene
JCL 16	BW25113/ F' [*traD36, proAB*+, *lacI*^{q}*ZΔM15* (Tet^R)]	(Atsumi et al., 2008a)
KS 145	JCL16 Δ*ilvB* Δ*ilvI*	(Atsumi and Liao, 2008)
CRS 39	JCL16 Δ*metA* Δ*tdh* Δ*ilvB* Δ*ilvI* Δ*adhE* Δ*leuABCD*	This study
CRS 40	JCL16 Δ*metA* Δ*tdh* Δ*ilvB* Δ*ilvI* Δ*adhE* Δ*leuABCD* Δ*poxB*	This study
CRS 43	JCL16 Δ*metA* Δ*tdh* Δ*ilvB* Δ*ilvI* Δ*adhE* Δ*leuABCD* Δ*iclR*	This study
CRS 44	JCL16 Δ*metA* Δ*tdh* Δ*ilvB* Δ*ilvI* Δ*adhE* Δ*leuABCD* Δ*poxB* Δ*pta*	This study
CRS 45	JCL16 Δ*metA* Δ*tdh* Δ*ilvB* Δ*ilvI* Δ*adhE* Δ*leuABCD* Δ*pta*	This study
CRS 47	JCL16 Δ*metA* Δ*tdh* Δ*ilvB* Δ*ilvI* Δ*adhE* Δ*leuABCD* Δ*arcA*	This study
CRS 59	JCL16 Δ*ilvB* Δ*ilvI* Δ*leuA*	This study
CRS 60	JCL16 Δ*ilvB* Δ*ilvI* Δ*leuA* Δ*avtA*	This study
CRS 61	JCL16 Δ*ilvB* Δ*ilvI* Δ*leuA* Δ*tdcE*	This study
CRS 62	JCL16 Δ*ilvB* Δ*ilvI* Δ*leuA* Δ*poxB*	This study
CRS 63	JCL16 Δ*ilvB* Δ*ilvI* Δ*leuA* Δ*thrB*	This study
CRS 64	JCL16 Δ*ilvB* Δ*ilvI* Δ*leuA* Δ*gltA*	This study
CRS 68	JCL16 Δ*ilvB* Δ*ilvI* Δ*leuA* Δ*pta* Δ*ldhA* Δ*adhE* Δ*frdA*	This study
CRS 69	JCL16 Δ*ilvB* Δ*ilvI* Δ*leuA* Δ*avtA* Δ*tdcE*	This study
CRS 70	JCL16 Δ*metA* Δ*tdh* Δ*ilvB* Δ*ilvI* Δ*adhE* Δ*leuABCD* Δ*gltA*	This study
CRS-SYN 2	CRS63/pSA138 + pAFC52	This study
CRS-SYN 3	CRS59/pSA138 + pAFC52	This study
CRS-SYN 6	CRS39/pAFC46 + pCS49	This study
CRS-SYN 7	CRS39/pAFC66 + pCS49	This study
CRS-SYN 12	CRS59/pAFC66 + pCS49 + pAFC52	This study
Plasmid	Genotype	Reference
pCS 31	P$_L$lacO$_1$:: *ilvA* (EC); p15A ori; Kan^R	This study
pCS 49	P$_L$lacO$_1$:: *thrA*^{fbr}*BC* (EC ATCC 21277); pSC101 ori; Spec^R	(Shen and Liao, 2008)
pCS 72	P$_L$lacO$_1$:: *ilvA* (EC)–*thrA*^{fbr}*BC* (EC ATCC 21277); p15A ori; Kan^R	This study
pCS 86	P$_L$lacO$_1$:: *gltA* (EC); pSC101 ori; Spec^R	This study
pSA 55I	P$_L$lacO$_1$:: *kivd* (LL)–*ADH2* (SC), *lacI*; ColE1 ori; Amp^R	(Shen and Liao, 2008)
pSA 138	P$_L$lacO$_1$:: *kivd* (LL)-*yqhD*(EC); ColE1 ori; Amp^R	(Atsumi and Liao, 2008)
pAFC 46	P$_L$lacO$_1$:: *kivd* (LL)–*ADH2* (SC)-*ilvA* (CG); ColE1 ori; Amp^R	(Cann and Liao, 2008)
pAFC 52	P$_L$lacO$_1$:: *cimA2*Δ (MJ)-*leuBCD*(EC); p15A ori; Kan^R	This study (from A.F. Cann)
pAFC 66	P$_L$lacO$_1$:: *kivd* (LL)-*yqhD* (EC)-*ilvA* (CG); ColE1 ori; Amp^R	This study (from A.F. Cann)
Primer	Sequence 5′→3′	Plasmid
gltA Acc65 f	TCAGGTACCATGGCTGATACAAAAGCAAAACTCACC	pCS86
gltA SalI r	TCAGTCGACTTAACGCTTGATATCGCTTTTAAAGTC	pCS86

2.3. Bacterial strains

E. coli BW25113 ($rrnB_{T14}$ $\Delta lacZ_{WJ16}$ *hsdR514* $\Delta araBAD_{AH33}$ $\Delta rhaBAD_{LD78}$) was designated as the wild-type (WT) (Datsenko and Wanner, 2000) for comparison. XL-1 Blue (Stratagene, La Jolla, CA) was used to propagate all plasmids. Construction of BW25113 F' (or JCL 16) was described in Atsumi et al. (2008a) to supply the $lacI^q$. The operon *leuABCD* was removed from strain CSR31 (Shen and Liao, 2008) using linear recombination described in Datsenko and Wanner (2000), creating CRS39. Host gene deletions of *pta*, *poxB*, *gltA*, *iclR*, and *arcA* were achieved with P1 transduction using the Keio collection strains (Baba et al., 2006) as donor and strain CRS39 and its derivatives as recipient.

The gene *leuA* was removed from strain KS145 (Atsumi and Liao, 2008) using linear recombination described in Datsenko and Wanner (2000). Host gene deletions of *avtA*, *tdcE*, *gltA*, *thrB*, *poxB*, *adhE*, *frdA*, *ldhA* and *pta* were achieved with P1 transduction using the Keio collection strains (Baba et al., 2006) as donor and strain CRS59 and its derivatives as recipient. The kan^R inserted into the target gene region was removed with pCP20 (Datsenko and Wanner, 2000) in between each consecutive knock out. Then, removal of the gene segment was verified by colony PCR using the appropriate primers.

2.4. Production media and cultivation condition

For 1-propanol production experiments, single colonies were picked from LB plates and inoculated into 2 mL of LB media contained in test tubes with the appropriate antibiotics (ampicillin 100 μg/mL, kanamycin 50 μg/mL, and spectinomycin 50 μg/mL). The overnight culture grown in LB at 37 °C in a rotary shaker (250 rpm) was then inoculated 1% (v/v) into 10 mL of M9 medium (6 g Na_2HPO_4, 3 g KH_2PO_4, 0.5 g NaCl, 1 g NH_4Cl, 1 mM $MgSO_4$, 1 mg vitamin B1 and 0.1 mM $CaCl_2$ per liter of water) containing 36 g/L glucose, 5 g/L yeast extract (BD Bacto, Franklin Lakes, NJ), appropriate antibiotics, and 1000X Trace Metal Mix A5 (2.86 g H_3BO_3, 1.81 g $MnCl_2 \cdot 4H_2O$, 0.222 g $ZnSO_4 \cdot 7H_2O$, 0.39 g $Na_2MoO_4 \cdot 2H_2O$, 0.079 g $CuSO_4 \cdot 5H_2O$, 49.4 mg $Co(NO_3)_2 \cdot 6H_2O$ per liter water) in 250 mL screwed-cap flasks. From this point on, cultivation of cells and production of 1-propanol were performed in the screwed-cap flasks, and the resulting state of oxygen limitation is referred to as the "micro-aerobic" condition. For productions which lasted more than 2 days, 72 g/L of glucose was used in the medium instead of 36 g/L. The culture was allowed to grow at 37 °C in a rotary shaker (250 rpm) to an OD_{600} of 0.4–0.6 then induced with 0.1 mM IPTG. An induction level of 1 mM was used when the production strain carried additional copies of *lacI* on the plasmid pSA55I. The induced cultures were grown at 30 °C in a rotary shaker. Samples were taken throughout the next few days by opening the screwed caps of the flasks, and culture broths were either centrifuged or filtered to retrieve the supernatant. In some experiments as indicated, 8 g/L of threonine or 2-ketobutyrate was fed directly to the production culture at 72 h. The pH of production culture dropped from 7 to between 5.5–6.5 in 24 h, depending on the strain used, and was re-adjusted back to 7 using 10 M NaOH everyday unless stated otherwise.

For the media exchange experiment, cells in the stationary phase which had stopped producing 1-propanol after a few days were spun down by ultracentrifugation at 4000 rpm under room temperature. The resulting cell pellet was resuspended with equal volumes of fresh M9 medium containing 72 g/L glucose, 5 g/L yeast extract, appropriate antibiotics, 1000X Trace Metal Mix A5, and 0.1 mM IPTG as described above. The resuspended culture in the 250 mL screwed-cap flasks was then placed back to the 30 °C shaker (250 rpm) and allowed to produce for the next few days. This process was iterated every 3 to 4 days.

2.5. Metabolite detections

The alcohol compounds were quantified by a gas chromatograph (GC) equipped with flame ionization detector. The system

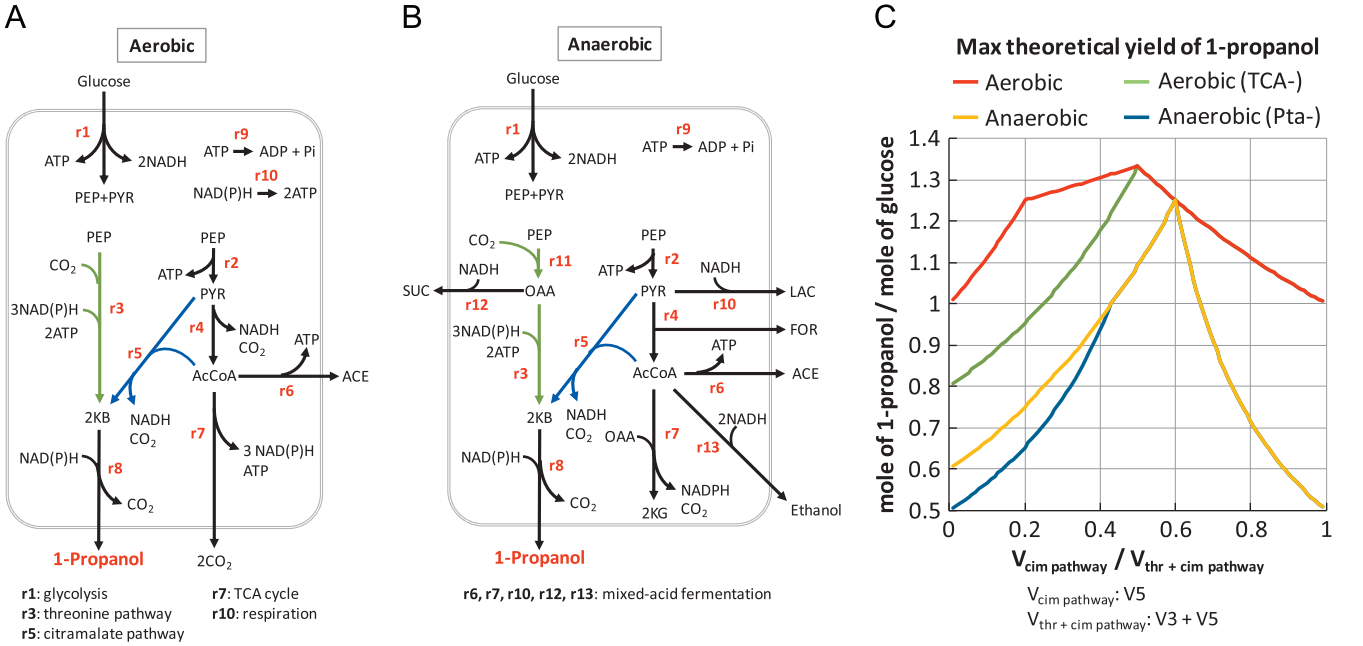

Fig. 2. Maximum theoretical yield calculations using stoichiometric flux balance (A), (B) 1-Propanol production network with the threonine pathway (denoted by green lines) and the citramalate pathway (denoted by blue lines) under aerobic and anaerobic condition. (C) Maximum theoretical yield of 1-propanol at different flux ratio of the threonine pathway and the citramalate pathway. Vi is defined as the flux of reaction ri. The *x*-axis represents flux fraction $V5/[V3+V5]$. 1-Propanol production yields using the dual pathway were analyzed under various scenarios as indicated by the legend. TCA—denotes deletion of the TCA cycle (reaction r7) in the aerobic network. Pta—denotes deletion of acetate synthesis from acetyl-CoA (reaction r6) in the anaerobic network. AcCoA, acetyl-CoA; PYR, pyruvate; PEP, phosphoenolpyruvate; OAA, oxaloacetate; 2KG, α-ketoglutarate; 2KB, 2-ketobutyrate; LAC, lactate; FOR, formate; ACE, acetate; SUC, succinate. (For interpretation of the references to color in this figure legend, the reader is referred to the web version of this article.)

consisted of model 5890A GC (Hewlett-Packard, Avondale, PA) and a model 7673A automatic injector, sampler and controller (Hewlett-Packard). Supernatant of culture broth was injected in split injection mode (1:15 split ratio) using 2-methyl-1-pentanol as the internal standard. Detailed procedures are described in Atsumi et al. (2008a). Glucose was quantified with a YSI glucose analyzer 2700. For other secreted metabolites, filtered supernatant was applied (0.02 mL) to an Agilent 1100 HPLC equipped with an auto-sampler (Agilent Technologies) and a BioRad (Biorad Laboratories, Hercules, CA) Aminex HPX87 column (5 mM H_2SO_4, 0.6 mL/min, column temperature at 35 °C). Organic acids were detected using a photodiode array detector at 210 nm. Concentrations were determined by extrapolation from standard curves.

2.6. Theoretical yield calculations

To calculate the maximum theoretical yield of 1-propanol from glucose, Excel with linear programming optimization was used. A set of mass balance equations describing all the relevant intracellular metabolites was established and was represented as $Sv=B$: where S is the stoichiometric matrix, with each column corresponding to a reaction in the network and each row containing the stoichiometric coefficient of each metabolite in the particular reaction. Vector v contains the molar fluxes for each reaction and their product, B, contains the rate of accumulation/depletion of each metabolite. The input glucose flux was set to 1, so that the yield of 1-propanol is equal to the 1-propanol production flux. We constructed S to represent the metabolic network consisting of glycolysis, TCA cycle, and the 1-propanol production pathways via threonine biosynthesis and the citramalate pathway under aerobic condition. At steady state, the rate of change of intracellular metabolite concentration is zero. Therefore, B is a column vector of zeros except for the row corresponding to the negative of glucose influx. Since S contains more reactions than metabolites (more columns than rows), it is under determined and can therefore be subject to optimization in order to find a solution. To calculate the maximum theoretical yield of 1-propanol, we performed linear optimization using the solver function in Excel (Supplementary materials). The objective function was set to maximize the 1-propanol flux while subject to the constraints ($Sv=B$, and the flux vector v greater than or equal to the lower bound which was set to 0). The ratio of flux from the threonine pathway and the citramalate pathway ($X=V_3/V_5$, Fig. 2a and b) was introduced as a constraint in the S matrix ($V_3-X\times V_5=0$). The flux fraction is then defined as the flux of citramalate pathway over the total flux going into 2-ketobutyrate ($F=V_5/[V_3+V_5]$), or $1/[X+1]$ if calculated from the flux ratio. With a subroutine written under Macros in Excel varying the flux fraction by the increment of 0.01, maximum yield of 1-propanol was automatically calculated by the solver for each flux fraction generated. The resulting yields were then plotted against the corresponding flux fraction. To use the macro, the contents were first enabled while opening the Excel program (click on "Options" from the pop-up security warning message and then "Enable this content"). Then, the network can be varied by adding or deleting certain reactions in the S matrix. Once the S matrix is modified to represent the target network, click on the "Macros" button under the "View" panel of Excel. Highlight the "ChangeRatio" program and then click "Run".

3. Results

3.1. Theoretical yield calculation identified synergy

The theoretical yield calculation was first performed with either the threonine pathway or the citramalate pathway individually using an Excel-based matrix optimization (Supplementary material). To calculate the theoretical yield, the overall reactions in each segment of the minimal pathway were first defined according to the lumped reactions as shown on Fig. 2a and b. Since the production of 1-propanol from glucose is not redox-balanced, the TCA cycle (r7) and the respiration (r10) were included in the aerobic network (Fig. 2a) to provide and recycle the reducing power and ATP. In anaerobic conditions, mixed acid fermentations (r6, r7, r10, r12, r13) were used to accomplish this task (Fig. 2b). It is worth noting that the NADH and NADPH were lumped as NAD(P)H for simplification purpose, which can be justified by the native activity of transhydrogenase in *E. coli* and the promiscuity of enzymes in the pathway towards NADH and NADPH. Similar approach has been taken previously in theoretical yield calculations without genome-scale modeling, such as the energetic analysis of non-photosynthetic CO_2-fixation pathways (Fast and Papoutsakis, 2012).

The synthesis of 1-propanol from glucose starts from glycolysis, which yields the following overall reaction:

$$\text{Glucose}\rightarrow \text{PEP}+\text{PYR}+2\ \text{NADH}+\text{ATP} \qquad (r1)$$

In this case, glucose is metabolized via the PTS-system, thus one mole of PEP is converted into one mole of pyruvate per glucose transported. Since gluconeogenesis does not occur in the present of glucose (Patnaik and Liao, 1994; Patnaik et al., 1995), the reaction of PEP to pyruvate is set to be irreversible in our network. If threonine pathway is used, one mole of CO_2 and PEP are incorporated into one mole of 2KB. Then, decarboxylation of 2KB into propylaldehyde losses one mole of CO_2. The net reaction is:

$$\text{PEP}+4\ \text{NAD(P)H}+2\ \text{ATP}\rightarrow \text{1-propanol} \qquad (r3+r8)$$

The net reaction from glucose to 1-propanol using the threonine pathway is thus:

$$\text{Glucose}+2\ \text{NAD(P)H}+\text{ATP}\rightarrow \text{1-propanol}+\text{PYR} \qquad (r1+r3+r8)$$

The amount of NAD(P)H and ATP needed for 1-propanol synthesis can be supplied by pyruvate oxidation via the TCA cycle. In this reaction scheme without gluconeogenesis, the maximum theoretical yield is 1 mol of 1-propanol produced per mole of glucose with the requirement of the TCA cycle. If the citramalate pathway is used for 1-propanol synthesis:

$$\text{Glucose}\rightarrow \text{PYR}+\text{AcCoA}+\text{CO}_2+3\ \text{NAD(P)H}+2\ \text{ATP} \qquad (r1+r2+r4)$$

$$\text{PYR}+\text{AcCoA}\rightarrow \text{1-propanol}+2\ \text{CO}_2 \qquad (r5+r8)$$

The net reaction becomes:

$$\text{Glucose}\rightarrow \text{1-propanol}+3\ \text{CO}_2+3\ \text{NAD(P)H}+2\ \text{ATP} \qquad (r1+r2+r4+r5+r8)$$

Thus, 1-propanol synthesis from glucose through the citramalate pathway also results in the maximum theoretical yield of 1 mol/mol, but is independent of the TCA cycle and is NAD(P)H and ATP surplus.

Thus, the citramalate pathway and the threonine pathway may complement each other through the cofactors. To investigate if synergy exists between the threonine pathway and the citramalate pathway in terms of 1-propanol yield, we performed a matrix-based maximum theoretical yield calculation using Excel with the minimal network for 1-propanol synthesis (Fig. 2a and b). The 1-propanol production flux was maximized using linear optimization under a given glucose flux, and the theoretical yield was calculated as the ratio of the two fluxes. The aerobic network (Fig. 2a) consisted of a PTS-dependent glucose uptake, glycolysis, TCA cycle, 1-propanol production via the threonine and/or the citramalate pathway and acetate synthesis. The pentose

phosphate pathway (PPP), which burns one carbon for the generation of two reducing equivalent, provides the same amount of reducing power as the TCA cycle and thus is not included in the minimal network. The maximum yield should remain the same whether the PPP or the TCA cycle is used to generate the necessary reducing power for threonine biosynthesis. The maximum theoretical yield of 1-propanol was examined by varying fractions of the citramalate pathway in the total flux going towards 2KB, which is represented by $V5/[V3+V5]$. As shown by the stoichiometric balances above, the maximum 1-propanol yield stayed at 1 mol/mol of glucose when only the threonine pathway or the citramalate pathway was present in the system (Fig. 2c, red line). As the two pathways were used together, 1-propanol theoretical yield increased and peaked at 1.33 mol/mol of glucose when equal amount of flux went through the threonine pathway and the citramalate pathway (Fig. 2c, red line).

Deletion of the ATP-forming acetate synthesis had no effect on the maximum theoretical yield of 1-propanol with either pathway aerobically. However, when the TCA cycle was removed from the system network, 1-propanol yield via the threonine pathway decreased by 20% to 0.8 mol/mol of glucose (Fig. 2c, green line). In this case, oxidation of pyruvate to acetate (instead of CO_2) was used to generate reducing power and ATP, thus explaining the carbon inefficiency. On the other hand, 1-propanol yield remained unaffected by deletion of the TCA cycle when citramalate pathway contributed more than 50% of the 2-ketobutyrate flux. This calculation demonstrates the importance of TCA cycle in 1-propanol synthesis via the threonine pathway. Coupling of cofactor utilizations in the dual pathway lowered the demand of TCA cycle for 1-propanol production and increased the maximum theoretical yield of 1-propanol under aerobic condition.

Next, we examined synergy of the threonine pathway and the citramalate pathway under anaerobic condition. The 1-propanol production network was altered partially by introduction of the mixed-acid fermentation pathways (lactate, acetate, formate, succinate, and ethanol). Maximum theoretical yield of 1-propanol dropped from 1 mol/mol of glucose to 0.6 mol/mol of glucose via the threonine pathway and 0.5 mol/mol of glucose using the citramalate pathway under anaerobic condition (Fig. 2c). The significant decrease of 1-propanol yield using the threonine pathway may be attributed to the limited pool of reducing power in the absence of TCA cycle. Contrary to the threonine pathway which was deficient on NAD(P)H, 1-propanol synthesis via the citramalate pathway generates a net of two NADH, which had to be recycled anaerobically via mixed-acid fermentation and led to the low 1-propanol yield. Deletion of the ATP-forming acetate synthesis further decreased 1-propanol yield via the threonine pathway while no effect was observed with the citramalate pathway.

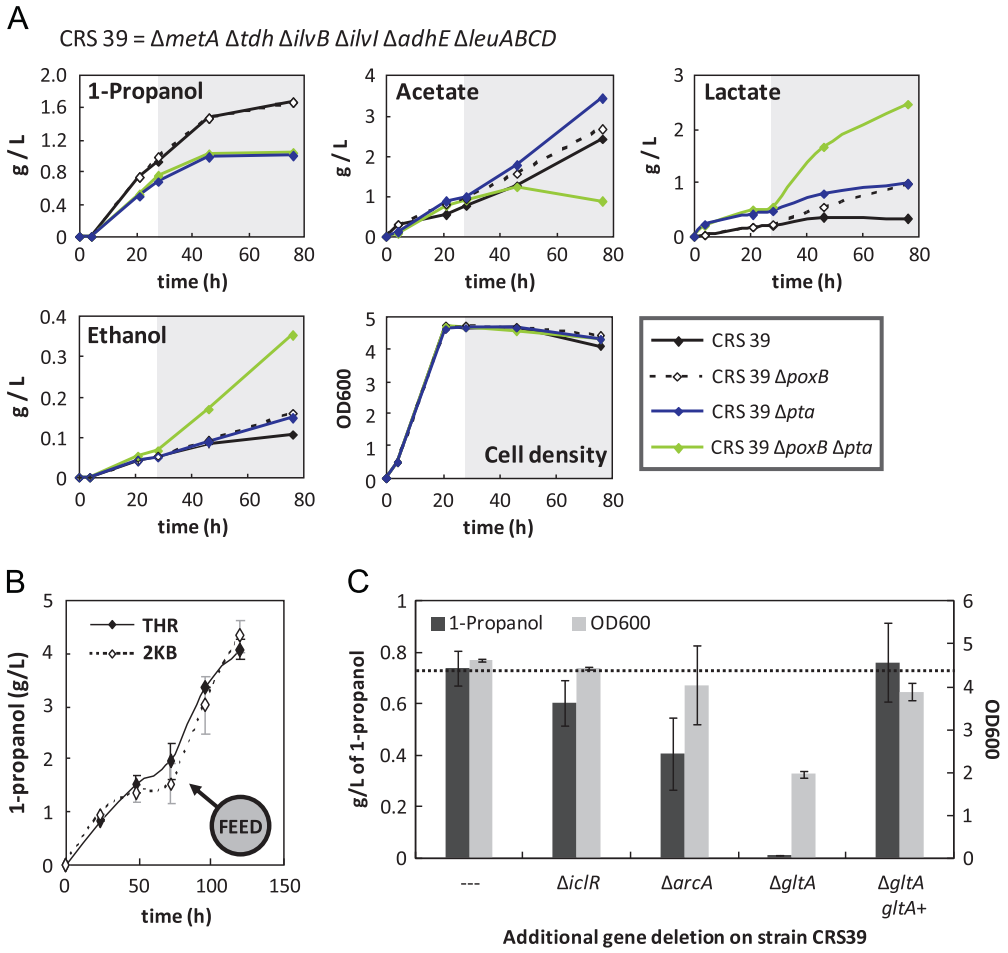

Fig. 3. Characterization of 1-propanol production via the threonine pathway. (A) Minimization of acetate formation and its effect on the distribution of metabolites. Acetate synthetic pathways were individually and simultaneously deleted from CRS39. All strains were transformed with plasmids pSA55I, pCS31, and pCS49. The switch from 1-propanol production to various fermentative byproducts is shaded in gray. Data values are an average of three independent repeats. Standard errors are within 25% of the averaged values. (B) Feeding of threonine (THR) or 2-ketobutyrate (2KB) at 72 h prolonged 1-propanol production. Time (h) indicates time since induction. (C) Significance of TCA cycle on 1-propanol production. Samples were taken after 24 h of induction. All strains carried plasmids pCS72 and pSA55I. "Δ" indicates gene deletion on top of CRS39. "+" indicates *gltA* overexpression from the plasmid pCS86 in addition to pCS72 and pSA55I. CRS39, JCL16 Δ*metA* Δ*tdh* Δ*ilvB* Δ*ilvI* Δ*adhE* Δ*leuABCD*.

Fig. 4. Synergistic effects of the dual pathway in 1-propanol yield, productivity, and titer as demonstrated from various engineered strains. (A) 1-Propanol yields and productivities were calculated within different time frames (since induction) during production phase as shown by the colored bars. 1-Propanol titer was measured at the 46 h since induction. Label "THR" and "threonine" indicates threonine pathway. Label "CIM" and "citramalate" indicates citramalate pathway. CHR represents presence of the native chromosomal genes (not overexpressed) and OVE denotes overexpression of the particular pathway on plasmids. (B) Time course of 1-propanol production, byproduct formation, cell density, and glucose consumption of selected strains. Genotypes of the strains tested (CRS-SYN 2, 3, 6, 7 and 12) are described in Table 1. Data values are an average of three independent repeats. Standard errors are within 15% of the averaged values.

Overall, synergy of the dual pathway in 1-propanol yield also exists anaerobically and resulted in an enhancement of the theoretical yield from 0.5 to 1.25 mol/mol of glucose.

In the following sections, we set out to construct *E. coli* strains with either individual pathways or dual pathway to validate the predicted synergy.

3.2. Characterization of 1-propanol production via the threonine pathway

To construct an *E. coli* 1-propanol strain using the threonine pathway, the chromosomal copy of LeuABCD responsible for the generation of 1-butanol precursor 2-ketovalerate was deleted (Fig. 1c). The resulting strain CRS39 (JCL 16 Δ*metA* Δ*tdh* Δ*ilvB* Δ*ilvI* Δ*adhE* Δ*leuABCD*), when transformed with plasmids pSA55I, pCS49 and pCS31 expressing *Lactococcus lactis Kivd*, *Saccharomyces cerevisiae ADH2*, *E. coli thrA*^{fbr}*BC*, and *ilvA* under the control of $P_L$lacO1 promoter, secreted 1-propanol but lost its ability to synthesize 1-butanol. 1-Propanol production followed a very similar profile as the previous co-producing strain (Shen and Liao, 2008), reaching a final titer of 1.5 to 2 g/L in three days under micro-aerobic condition with significant accumulation of acetate (>3 g/L) in the stationary phase (Fig. 3a). In this work, micro-aerobic condition is defined as the state of limited oxygen supply as a result of cultivation of cells in screwed-cap flasks.

To minimize carbon leakage into the by-product acetate, the major acetate production routes from acetyl-CoA and pyruvate catalyzed by phosphate acetyltransferase (Pta) and pyruvate oxidase (PoxB) were disrupted, respectively (Fig. 1b). Whereas single deletion of *pta* or *poxB* had no effect on acetate secretion, simultaneous removal of both *pta* and *poxB* successfully lowered acetate accumulation from 3 g/L to less than 1 g/L (Fig. 3a). It is important to note that while strain CRS40 (CRS39Δ*poxB*) demonstrated very similar production profile of 1-propanol and acetate compared to CRS39, deletion of *pta* (CRS39Δ*pta*) led to huge decrease of 1-propanol (Fig. 3a). This observation correlates with the result of the yield calculations (Fig. 2c), in which the ATP-forming acetate synthesis is important to supply ATP for threonine production under micro-aerobic/anaerobic condition. The significant drop of acetate formation in CRS44 (CRS39 Δ*pta* Δ*poxB*); however, did not improve 1-propanol production. 1-Propanol titer dropped 40% to 1 g/L while lactate secretion was elevated by 10-fold (0.25 to 2.5 g/L) compared to CRS39. Synthesis of 1-propanol from strain CRS39 plateaued after 72 h and could only be extended upon feeding of threonine or 2-ketobutyrate to the production culture (Fig. 3b). These observations suggest the existence of bottleneck(s) in the threonine pathway as oxygen level decreased in the culture flasks, which caused the pyruvate flux to stall in glycolysis and escape as fermentative products such as acetate, lactate and ethanol.

Significance of the TCA cycle in threonine biosynthesis was revealed when the citrate synthase encoded by *gltA* was deleted from CRS39 (Fig. 1b). Disruption of the TCA cycle upon elimination of *gltA* completely abolished the production of 1-propanol in strain CRS70 (JCL 16 Δ*metA* Δ*tdh* Δ*ilvB* Δ*ilvI* Δ*adhE* Δ*leuABCD* Δ*gltA*) (Fig. 3c) transformed with plasmids pSA55I ($P_L$lacO1:: *kivd ADH2*) and pCS72 ($P_L$lacO1:: *ilvA thrA*^{fbr}*BC*). The important role of the TCA cycle for 1-propanol production may lie in its supply of the essential cofactors (NADPH, ATP) and intermediate (glutamate) required in the threonine pathway (Fig. 1a and b). This result correlates with the theoretical yield calculations (Fig. 2c) although a much stronger effect was observed in the experiment upon disruption of the TCA cycle (Δ*gltA*). Overexpression of GltA under $P_L$lacO1 promoter on plasmid pCS86 complemented the Δ*gltA* phenotype of CRS70 and completely restored 1-propanol production when co-transformed with pSA55I and pCS72 (Fig. 3c). Deletion of the major anaerobic transcriptional repressor of GltA encoded by *arcA* decreased 1-propanol titer by 50% in CRS47 (JCL 16 Δ*metA* Δ*tdh* Δ*ilvB* Δ*ilvI* Δ*adhE* Δ*leuABCD* Δ*arcA*), which may be a pleiotropic effect upon removal of the global regulator (Fig. 3c). Activation of the glyoxylate shunt by knocking out its transcriptional repressor encoded by *iclR* decreased the level of 1-propanol production by 20% in CRS43 (JCL 16 Δ*metA* Δ*tdh* Δ*ilvB* Δ*ilvI* Δ*adhE* Δ*leuABCD* Δ*iclR*) (Fig. 3c). Even though usage of the glyoxylate shunt circumvents a decarboxylation step and minimizes carbon loss (Lee et al., 2007), bypass of the NAD(P)H and ATP-generation steps might be detrimental for the threonine-derived 1-propanol synthesis under micro-aerobic condition.

3.3. Experimental data verified synergy of the dual pathway

To verify the synergistic effects in 1-propanol production as predicted by the yield calculations, we examined the 1-propanol production profile from *E. coli* strains overexpressing the threonine pathway and/or the citramalate pathway simultaneously or individually (Fig. 4a). Strain CRS39 (JCL 16 Δ*metA* Δ*tdh* Δ*ilvB* Δ*ilvI* Δ*adhE* Δ*leuABCD*) harboring plasmids pAFC46 ($P_L$lacO1:: *kivd ADH2 ilvA*) and pCS49 ($P_L$lacO1:: *thrA*^{fbr}*BC*) was used to synthesize 1-propanol via the threonine pathway while strain CRS63 (JCL16 Δ*ilvB* Δ*ilvI* Δ*leuA* Δ*thrB*) transformed with plasmids pAFC52 ($P_L$lacO1:: *cimA2*Δ *leuBCD*) and pSA138 ($P_L$lacO1:: *kivd yqhD*) was used to synthesize 1-propanol via the citramalate pathway. Disruption of the *E. coli* native threonine pathway was performed to eliminate contribution of the native threonine pathway to the production of 2-ketobutyrate. The homoserine kinase encoded by *thrB* was chosen as the knock-out candidate for its lack of isozymes in contrast to the other essential enzymes such as ThrA or IlvA (Fig. 1a). Overexpression of both threonine pathway and citramalate pathway was achieved by transforming strain CRS59 (JCL16 Δ*ilvB* Δ*ilvI* Δ*leuA*) with plasmids pAFC52, pCS49, and pAFC66 ($P_L$lacO1:: *kivd yqhD ilvA*). Strain CRS59 carrying plasmid pAFC52, pSA138 and native chromosomal copy of the threonine/2-ketobutyrate biosynthetic genes was also constructed to assess the necessity of threonine pathway overexpression to achieve the predicted synergy.

1-Propanol yields from the four strains were calculated with respect to different time frames during production to take into consideration of the potential influence of biomass formation on product yield. As shown in Fig. 4a, comparison of 1-propanol production yield among different strains demonstrated the synergy of threonine pathway and citramalate pathway in 1-propanol synthesis across all time frames. 1-Propanol yield reached about 0.15 g/g of glucose under micro-aerobic condition when both pathways were overexpressed simultaneously. Interestingly, similar synergistic effect was also observed from the strain overexpressing the citramalate pathway coupled with native activity of the threonine pathway. On the other hand, overexpression of threonine pathway or citramalate pathway alone resulted in a lower 1-propanol yield of about 0.09 to 0.11 g/g of glucose respectively (Fig. 4a). It is interesting to note that the citramalate pathway supported slightly higher 1-propanol yield compared to the threonine pathway, which agrees with the theoretical yield calculations if one considers the impaired TCA cycle activity under micro-aerobic condition (Fig. 2c). Overall, synergy of the dual pathway improved 1-propanol yield by 30% to 50% compared to using the citramalate pathway or the threonine pathway alone, which correlates well with the predictions made by the yield model.

Interestingly, coupling of the threonine pathway and the citramalate pathway also improved the rate of 1-propanol synthesis significantly. Production of 1-propanol followed similar profile in strains overexpressing only the threonine pathway or citramalate pathway,

reaching a productivity of 1 g/L/day and an OD of about 4.5 (Fig. 4b). On the other hand, overexpression of both pathways on plasmids resulted in almost identical yield and production titer as overexpression of only the citramalate pathway coupled with native activity of the threonine pathway (Fig. 4). We therefore reason that the increase in yield and productivity is due to synergy of the two pathways and not due to more enzymes working towards the product. 1-Propanol productivity was improved to 2.5 g/L/day by synergy of the dual pathway while cell density increased a bit to an OD of 5.5. Overall, synergy of the dual pathway improved 1-propanol productivity by about three fold. Production of 1-propanol continued after cells entered stationary phase and maintained consistent yield and rate within the 48 h production period (Fig. 4b). It is worth noting that overexpression of the NADPH-dependent alcohol dehydrogenase YqhD for 1-propanol synthesis using only the threonine pathway led to significantly lower yield and productivity compared to overexpression of the NADH-dependent ADH2 (Fig. 4a). Since previously ADH2 was reported to be insoluble in *E. coli* (Atsumi etal., 2010), the native alcohol dehydrogenase may contribute to the observed 1-propanol production. On the other hand, higher and more consistent production of 1-propanol was achieved with YqhD overexpression whenever citramalate pathway is functional in the system. This observation suggests the deficiency of NADPH under micro-aerobic condition to support 1-propanol synthesis using only the threonine pathway.

3.4. Characterization of 1-propanol production from the synergistic dual pathway

To characterize 1-propanol production from the dual pathway, various genes were deleted in strain CRS59 to study their effects on the synthesis of 1-propanol (Fig. 5a). Threonine pathway was not overexpressed due to the similar 1-propanol yield and productivity obtained with and without its overexpression (Fig. 4). Contrary to the 1-propanol production using only threonine pathway (Fig. 3c), disruption of the TCA cycle upon deletion of *gltA* (CRS64) had no significant effect on the dual pathway for its efficiency to generate 2-ketobutyrate. This observation verified the prediction by the theoretical yield calculations where TCA cycle is essential for 1-propanol production using the threonine pathway but insignificant if coupled to the citramalate pathway. Whereas *gltA* knock-out completely abolished 1-propanol production via threonine biosynthesis (Fig. 3c), it only resulted in 30% drop of 1-propanol titer when citramalate pathway is present, reaching 4.5 g/L in 72 h with a slightly lowered cell density (Fig. 5a).

To attempt at further increasing the 1-propanol productivity and titer, pathways that compete for the essential precursor 2-ketobutyrate were deleted in strain CRS59 (Fig. 1c). Elimination of the 2-ketobutyrate aminotransferase encoded by *avtA* or the 2-ketobutyrate formate-lyase encoded by *tdcE* released 2-ketobutyrate from undesirable side reactions but yielded no significant improvement in 1-propanol production, at most reaching a titer of 7.5 g/L in three days (Fig. 5a). Surprisingly, adverse effect was observed when the two knock-outs were combined in strain CRS59. The strain CRS69 (JCL16 Δ*ilvB* Δ*ilvI* Δ*leuA* Δ*avtA* Δ*tdcE*) transformed with plasmids pAFC52 and pSA138 only accumulated about 2 g/L of 1-propanol in 72 h, which was 65% lower than the amount secreted by the base strain CRS59 (Fig. 5a). Accumulation of 2-ketobutyrate may be toxic to cells (Larossa and Vandyk, 1987) if the turnover rate into 1-propanol by Kivd and YqhD is not high enough.

Deletion of the aerobic pyruvate metabolism pathway catalyzed by PoxB (strain CRS62) to conserve the essential precursor

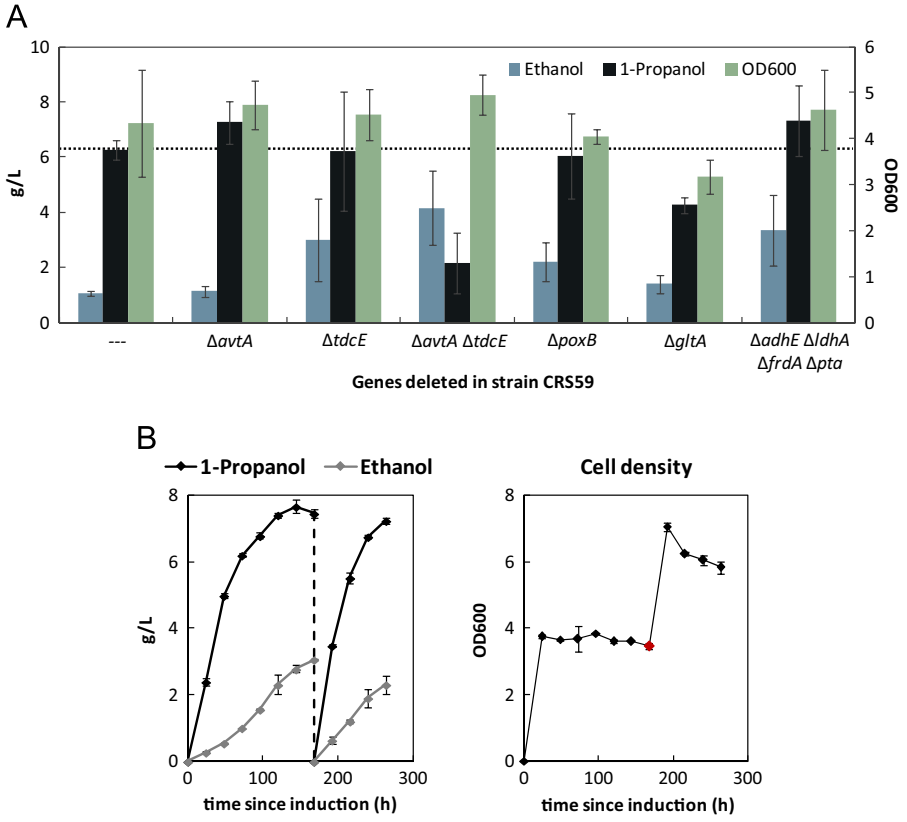

Fig. 5. Characterization of 1-propanol production from the synergistic dual pathway. (A) Deletion analysis of 1-propanol production with overexpression of the citramalate pathway and native chromosomal copy of the threonine pathway. CRS59 was used as the base strain for the additional gene knock-outs. Samples were taken after 72 h of fermentation. 1-Propanol titer produced by the base strain CRS59 is highlighted with the black dashed line. All strains contained plasmids pAFC52 and pSA138. (B) Continuous production of 1-propanol achieved via media exchange. Strain CRS59 transformed with plasmids pAFC52 and pSA138 was used. Cells were spun down and resuspended with equal volumes of fresh production media as indicated by the dashed line on the production figure or the red dot on the cell growth figure. CRS59, JCL16 Δ*ilvB* Δ*ilvI* Δ*leuA*. (For interpretation of the references to color in this figure legend, the reader is referred to the web version of this article.)

for the initiation of ketoacid elongation had no significant effect on the 1-propanol production (Fig. 5a). To examine 1-propanol production using a pyruvate and acetyl-CoA accumulating host, mixed-acid fermentation pathways catalyzed by *AdhE*, *LdhA*, *Frd*, and *Pta* were simultaneously deleted in strain CRS59, resulting in CRS68 (JCL16 Δ*ilvB* Δ*ilvI* Δ*leuA* Δ*adhE* Δ*ldhA* Δ*frdA* Δ*pta*). Elimination of competing pathways for the citramalate precursors redirected slightly more carbon flux into the citramalate pathway and increased the 1-propanol titer by 20%, reaching 8 g/L in 72 h (Fig. 5a). However, the gene deletions also resulted in greater variation of 1-propanol titers produced among individual clones.

Micro-aerobic production of 1-propanol via synergy of the dual pathway in strain CRS59 transformed with plasmids pAFC52 and pSA138 still plateaued around 7.5 g/L with adjustment of culture pH and could not be extended upon addition of glucose. As shown in Fig. 5b, resuspension of cells in fresh medium allowed 1-propanol production to continue with an average productivity of 2–3 g/L/day. With the serial exchange of fresh medium, 1-propanol production went on for 11 days without any sign of recession. This result reveals that the presence of toxic metabolites and/or the depletion of essential compounds in the culture broth played a major role in the plateau of 1-propanol production via the coupled pathway.

4. Discussion

In this work, we have demonstrated the synergy between the threonine pathway and the citramalate pathway for 1-propanol production. The synergy was predicted by a yield calculation model and verified experimentally in *E. coli*. The complementary nature of the two pathways in terms of oxygen requirement, redox balance, carbon efficiency, and ATP demand was revealed through the theoretical yield calculations. Coupling of the complementary driving force demands originated from the synergistic nature of the individual pathway enabled significant improvement in 1-propanol productivity and yield, reaching 8 g/L at 2.5 g/L/day and 0.15 g/g of glucose.

Both the threonine pathway and the citramalate pathway are part of the 2-ketoacid pathway network involved in amino acid biosynthesis (Fig. 1a). Production of desirable compounds from the ketoacid pathway is amendable to directed evolution based on auxotrophic growth selections and amino acid analogues (Smith and Liao, 2011). Whether the threonine hyper-producers were created by rational design or random mutagenesis, one common requirement for microbial threonine production in the fed-batch fermentation process is high aeration (Lee et al., 2007; Shiio et al., 1971). As shown by the theoretical yield calculations, full TCA cycle activity granted by sufficient oxygen supply is necessary to meet the high demand of reducing power and ATP by the threonine biosynthetic pathway. Two molecules of NAD(P)H are consumed for the formation of homoserine from aspartyl-4-phosphate while one NADPH is required for the conversion of 2-ketoglutarate back to glutamate (Fig. 1a). Requirement of glutamate as the NH_3 donor for the transamination reaction catalyzed by AspC may be another reason for the necessity of TCA cycle in threonine production. A total of three NAD(P)H and two ATP are required for the synthesis of one threonine molecule. TCA cycle along with pyruvate dehydrogenase are the major providers of NAD(P)H, whose activities are regulated and repressed under micro-aerobic conditions (Kang et al., 2005; Kim et al., 2008; Peng and Shimizu, 2003). Alternatively, the pentose phosphate pathway provides the same amount of reducing equivalent as the TCA cycle (2 NAD(P)H per carbon burned); however, it is also heavily regulated by the host anaerobically. In addition, activity of the pyridine nucleotide transhydrogenase for the inter-conversion of NADH into NADPH drops when oxygen supply becomes limited (Sauer et al., 2004). As a result, synthesis of threonine and its downstream products under oxygen-limiting conditions is difficult due to limited cofactor pool. Requirement of high aeration often results in higher operational costs and limits the theoretical yield due to burning of carbon through the TCA cycle.

Contrary to the threonine pathway, the citramalate pathway requires no ATP and generates a net of one NADH, which can potentially supply any other pathway that is redox-limited (Fig. 1a). It represents the ideal route to make 2-ketobutyrate under oxygen-limiting conditions when the pyruvate dehydrogenase and the TCA cycle are inefficient to supply the reducing power and substrate needed for threonine production. However, as demonstrated by the theoretical yield calculations, complete anaerobic condition is also detrimental to 1-propanol production via the citramalate pathway due to carbon leakage into fermentation byproducts for the recycling of excess NADH. The intrinsic redox features associated with each pathway therefore limit the 1-propanol productivity and yield that can be reached under a distinct operating condition. As predicted by the theoretical yield calculations, utilization of both threonine pathway and citramalate pathway at a flux ratio of 1:1 and 1:1.5 maximized 1-propanol yields under aerobic and anaerobic condition respectively, revealing the synergistic nature of the two pathways. It takes one pyruvate and one acetyl-CoA to make one molecule of 2KB via the citramalate pathway whereas only one PEP is required to synthesize one 2KB from the threonine pathway. Therefore, it is important to point out that a flux ratio of 1:1 between the threonine pathway and the citramalate pathway at the maximum 1-propanol yield implies 2/3 of the glucose flux going into the citramalate pathway and 1/3 going into the threonine pathway.

The model-aided design of 1-propanol production system based on synergy of the dual pathway successfully coupled the driving forces present in each pathway and led to more than two-fold increase in 1-propanol productivity and 50% increase in yield micro-aerobically. On the other hand, production of 1-propanol using only the threonine pathway or the citramalate pathway resulted in lower yield, productivity, and titer, parallel to the predictions made by the theoretical yield calculations. Disruption of the native threonine pathway by deletion of the host gene *thrB* may have caused intracellular accumulation of the intermediate homoserine, which can potentially lead to cell toxicity. Construction of a modified 1-propanol biosynthetic pathway via the formation of propinyl-CoA utilizing both threonine pathway and the citramalate pathway has also been reported recently (Jun Choi et al., 2012). The resulting yield and productivity of 1-propanol from glucose also agrees with the synergistic effects as shown by the theoretical yield calculations and experimental verifications in this study. In this work, the use of PTS-system for glucose transport in the yield model lowered the maximum theoretical yield of 1-propanol from the threonine pathway (1 mol of 1-propanol/mole of glucose) compared to the 1.2 mol/mol calculated when glucose internalization is decoupled from PEP consumption. Since gluconeogenesis does not occur in the presence of glucose (Patnaik and Liao, 1994; Patnaik et al., 1995), the irreversibility of PEP to pyruvate limited the maximum yield of 1-propanol that can be obtained via the threonine pathway. Overexpression of Pps to convert pyruvate back into PEP (Chao and Liao, 1994; Patnaik et al., 1992) or cloning of GalP/Glk to utilize the non-PTS mechanism for glucose uptake and phosphorylation (Hernandez-Montalvo et al., 2003) are potential ways to enhance the theoretical yield of products originating from PEP.

The inherent redox nature of threonine pathway and citramalate pathway complements each other and drives carbon flux into

the common intermediate 2-ketobutyrate via the dual pathway. Although the last decarboxylation step catalyzed by LeuB is carbon-wasteful, it may serve as a driving force to pull fluxes into the citramalate pathway, which in turn drives the threonine pathway by the net generation of reducing power. Utilization of such synergistic pathways improves versatility of production condition and has been demonstrated in the biosynthesis of succinate by combining glyoxylate shunt and the oxidative branch of the TCA cycle (Lin et al., 2005). The work presented here highlights the significance of synergy in pathway design and its potential application towards improving the production rate and yield of target chemicals. Exploration of complementary nature in individual pathways will facilitate identification of more synergistic pathways, which can be applied as a design principle to enhance production efficiency via metabolic engineering.

Acknowledgments

This work was supported in part by the NSF MCB-1139318 and the UCLA-DOE Institute for Genomics and Proteomics. The authors thank Anthony F. Cann for the plasmids, and Ethan I. Lan and Jimmy G Lafontaine Rivera for their valuable discussions.

Appendix A. Supporting information

Supplementary data associated with this article can be found in the online version at http://dx.doi.org/10.1016/j.ymben.2013.01.008.

References

Atsumi, S., Cann, A.F., Connor, M.R., Shen, C.R., Smith, K.M., Brynildsen, M.P., Chou, K.J., Hanai, T., Liao, J.C., 2008a. Metabolic engineering of *Escherichia coli* for 1-butanol production. Metab. Eng. 10, 305–311.

Atsumi, S., Hanai, T., Liao, J.C., 2008b. Non-fermentative pathways for synthesis of branched-chain higher alcohols as biofuels. Nature 451, 86–89.

Atsumi, S., Liao, J.C., 2008. Directed evolution of *Methanococcus jannaschii* citramalate synthase for biosynthesis of 1-propanol and 1-butanol by *Escherichia coli*. Appl. Environ. Microbiol. 74, 7802–7808.

Atsumi, S., Wu, T.Y., Eckl, E.M., Hawkins, S.D., Buelter, T., Liao, J.C., 2010. Engineering the isobutanol biosynthetic pathway in *Escherichia* coli by comparison of three aldehyde reductase/alcohol dehydrogenase genes. Appl. Microbiol. Biotechnol 85, 651–657.

Baba, T., Ara, T., Hasegawa, M., Takai, Y., Okumura, Y., Baba, M., Datsenko, K.A., Tomita, M., Wanner, B.L., Mori, H., 2006. Construction of *Escherichia coli* K-12 in-frame, single-gene knockout mutants: the Keio collection. Mol. Syst. Biol. 2 (2006), 0008.

Bond-Watts, B.B., Bellerose, R.J., Chang, M.C.Y., 2011. Enzyme mechanism as a kinetic control element for designing synthetic biofuel pathways. Nat. Chem. Biol. 7, 222–227.

Cann, A.F., Liao, J.C., 2008. Production of 2-methyl-1-butanol in engineered *Escherichia coli*. Appl. Microbiol. Biotechnol. 81, 89–98.

Chao, Y.P., Liao, J.C., 1994. Metabolic responses to substrate futile cycling in *Escherichia coli*. J. Biol. Chem. 269, 5122–5126.

Datsenko, K.A., Wanner, B.L., 2000. One-step inactivation of chromosomal genes in *Escherichia coli* K-12 using PCR products. Proc. Nat. Acad. Sci. U.S.A. 97, 6640–6645.

Dellomonaco, C., Clomburg, J.M., Miller, E.N., Gonzalez, R., 2011. Engineered reversal of the beta-oxidation cycle for the synthesis of fuels and chemicals. Nature 476, 355–359.

Fast, A.G., Papoutsakis, E.T., 2012. Stoichiometric and energetic analyses of non-photosynthetic CO2-fixation pathways to support synthetic biology strategies for production of fuels and chemicals. Curr. Opin. Chem Eng. 1, 380–395.

Hernandez-Montalvo, V., Martinez, A., Hernandez-Chavez, G., Bolivar, F., Valle, F., Gosset, G., 2003. Expression of galP and glk in a *Escherichia coli* PTS mutant restores glucose transport and increases glycolytic flux to fermentation products. Biotechnol. Bioeng. 83, 687–694.

Iso, M., Chen, B.X., Eguchi, M., Kudo, T., Shrestha, S., 2001. Production of biodiesel fuel from triglycerides and alcohol using immobilized lipase. J. Mol. Catal. B: Enzym. 16, 53–58.

Jain, R., Yan, Y., 2011. Dehydratase mediated 1-propanol production in metabolically engineered *Escherichia coli*. Microb. Cell Fact. 10, 97.

Jun Choi, Y., Hwan Park, J., Yong Kim, T., Yup Lee, S., 2012. Metabolic engineering of *Escherichia coli* for the production of 1-propanol. Metab. Eng. 14, 477–486.

Kang, Y.S., Weber, K.D., Yu, Q., Kiley, P.J., Blattner, F.R., 2005. Genome-wide expression analysis indicates that FNR of *Escherichia coli* K-12 regulates a large number of genes of unknown function. J. Bacteriol. 187, 1135–1160.

Kim, Y., Ingram, L.O., Shanmugam, K.T., 2008. Dihydrolipoamide dehydrogenase mutation alters the NADH sensitivity of pyruvate dehydrogenase complex of *Escherichia coli* K-12. J. Bacteriol. 190, 3851–3858.

Lan, E.I., Liao, J.C., 2011. Metabolic engineering of cyanobacteria for 1-butanol production from carbon dioxide. Metab. Eng. 13, 353–363.

Lan, E.I., Liao, J.C., 2012. ATP drives direct photosynthetic production of 1-butanol in cyanobacteria. Proc. Nat. Acad. Sci. U.S.A. 109, 6018–6023.

Lan, E.I., Liao, J.C. Microbial synthesis of n-butanol, isobutanol, and other higher alcohols from diverse resources. Bioresour. Technol., http://dx.doi.org/10.1016/j.bbr.2011.03.031, in press.

Larossa, R.A., Vandyk, T.K., 1987. Metabolic mayhem caused by 2-ketoacid imbalances. Bioessays 7, 125–130.

Lee, K.H., Park, J.H., Kim, T.Y., Kim, H.U., Lee, S.Y., 2007. Systems metabolic engineering of *Escherichia coli* for L-threonine production. Mol. Syst. Biol. 3, 149.

Lin, H., Bennett, G.N., San, K.Y., 2005. Metabolic engineering of aerobic succinate production systems in *Escherichia coli* to improve process productivity and achieve the maximum theoretical succinate yield. Metab. Eng. 7, 116–127.

Patnaik, R., Liao, J.C., 1994. Engineering of *Escherichia coli* central metabolism for aromatic metabolite production with near theoretical yield. Appl. Environ. Microbiol. 60, 3903–3908.

Patnaik, R., Roof, W.D., Young, R.F., Liao, J.C., 1992. Stimulation of glucose catabolism in *Escherichia coli* by a potential futile cycle. J. Bacteriol. 174, 7527–7532.

Patnaik, R., Spitzer, R.G., Liao, J.C., 1995. Pathway engineering for production of aromatics in *Escherichia coli*: confirmation of stoichiometric analysis by independent modulation of AroG, TktA, and Pps activities. Biotechnol. Bioeng. 46, 361–370.

Peng, L., Shimizu, K., 2003. Global metabolic regulation analysis for *Escherichia coli* K12 based on protein expression by 2-dimensional electrophoresis and enzyme activity measurement. Appl. Microbiol. Biot. 61, 163–178.

Sauer, U., Canonaco, F., Heri, S., Perrenoud, A., Fischer, E., 2004. The soluble and membrane-bound transhydrogenases UdhA and PntAB have divergent functions in NADPH metabolism of *Escherichia coli*. J. Biol. Chem. 279, 6613–6619.

Shen, C.R., Lan, E.I., Dekishima, Y., Baez, A., Cho, K.M., Liao, J.C., 2011. Driving forces enable high-titer anaerobic 1-butanol synthesis in *Escherichia coli*. Appl. Environ. Microb. 77, 2905–2915.

Shen, C.R., Liao, J.C., 2008. Metabolic engineering of *Escherichia coli* for 1-butanol and 1-propanol production via the keto-acid pathways. Metab. Eng. 10, 312–320.

Shen, C.R., Liao, J.C., 2011. A synthetic iterative pathway for ketoacid elongation. Methods Enzymol. 497, 469–481.

Shiio, I., Nakamori, S., Sano, K., Fermentation production of l-threonine. Vol. 3580810, U.S. Patent 3580810, 1971.

Smith, K.M., Liao, J.C., 2011. An evolutionary strategy for isobutanol production strain development in *Escherichia coli*. Metab. Eng. 13, 674–681.

Tseng, H.C., Harwell, C.L., Martin, C.H., Prather, K.L., 2010. Biosynthesis of chiral 3-hydroxyvalerate from single propionate-unrelated carbon sources in metabolically engineered *E. coli*. Microb. Cell Fact. 9, 96.

Zhang, K., Sawaya, M.R., Eisenberg, D.S., Liao, J.C., 2008. Expanding metabolism for biosynthesis of nonnatural alcohols. Proc. Nat. Acad. Sci. U.S.A. 105, 20653–20658.